# Adaptive Link-by-Link Band Allocation: A Novel Adaptation Scheme in Multi-Band Optical Networks

Masahiro Nakagawa, Hiroki Kawahara, Takeshi Seki, Takashi Miyamura
*NTT Network Service Systems Laboratories*
*NTT Corporation*
3-9-11, Midori-cho, Musashino-shi, Tokyo, 180-8585, Japan
masahiro.nakagawa.wh@hco.ntt.co.jp

***Abstract*—Multi-band optical networking is a viable solution to deal with ever-increasing traffic demands using existing fiber infrastructure. To unleash the full potential of such a solution, available spectrum resources must be efficiently utilized in consideration of the attainable transmission quality and margin. In this paper, we propose a novel optical-layer adaptation scheme for low-margin multi-band optical networking. With our scheme, the transmission bands can be adapted link-by-link in consideration of transmission quality, which can efficiently reduce margins and improve network performance. Simulation results demonstrate that the proposed adaptation scheme enables a significant increase in the traffic volume that can be accommodated.**

***Keywords—multi-band optical network, transmission quality, low-margin networking, adaptation, band allocation, wavelength-selective band switching***

## I. INTRODUCTION

Rapid evolution of broadband access technologies and bandwidth intensive applications have pushed the growth of network traffic volume. This ongoing trend has been driving the need for further capacity on transport networks. Accordingly, enhancing available capacity while keeping network costs under control is of great importance for network operators. Recently, multi-band (MB) optical networking has attracted much attention as a viable solution to cost-effectively expand network capacity [1–4]. On MB networks, the available optical spectrum can be naturally increased in contrast to traditional single-band operations (e.g., C-band only), which offers a high potential for network capacity expansion using existing fiber infrastructure.

To unleash the full potential of MB operations, available spectrum resources must be efficiently utilized in consideration of transmission quality, which is often expressed by the generalized signal-to-noise ratio (GSNR). Moreover, GSNR performance and the effective available capacity are strongly affected by optical parameters and nonlinear effects that include stimulated Raman scattering (SRS). Note that SRS causes a power transition from shorter to longer wavelengths with fiber propagation, and its impact must be well managed in MB operations. Although power tilt over multiple transmission bands can be compensated by power equalizing techniques at the end of each span or node hop, the accumulated amount of GSNR degradation can vary because of variation in optical parameters such as fiber attenuation and amplifier noise figure. This may lead to GSNR performance variation depending not only on the path length but also on the band. It should be noted that a fiber launch power optimization method has been investigated for balancing GSNR performance over multiple bands [5]. However, such a method inevitably causes degradation in GSNR values on better-performing bands. In [5], in fact, a remarkable degradation in GSNR performance of the best-performing band can be found, which can lead to insufficient transmission quality (i.e., margin shortage) when provisioning a long-distance path in a large-scale network. Also note that both margin shortage and high margins (resulting from GSNR performance variation) can severely limit network capacity [6], forcing network operators to rethink margin management strategies. Furthermore, low-margin operations on MB networks is key for maximizing network capacity.

Adaptivity in the optical layer is crucial to attain lower margins while efficiently utilizing spectrum resources. In fact, the modulation format adaptation scheme has become common for high-capacity optical networks [7]. In this scheme, transponders (TRs) can adjust GSNR threshold required for error-free operation by changing the modulation format according to the received GSNR, which can suppress margins. Additionally, we can also adaptively allocate a band to each path [8], whereas an end-to-end band adaptation scheme only offers the capability to select received GSNR from those for each band on a particular route. Moreover, since conventional schemes generally utilize limited numbers of discrete GSNR threshold and/or received GSNR, margin adaptation has only been achieved with coarse granularity so far. Therefore, the abovementioned trends and facts necessitate a new adaptation approach to enable fine-granularity margin reduction while avoiding margin shortage even on large-scale networks.

In this paper, we propose an adaptive link-by-link band allocation scheme that utilizes the wavelength-selective band switching that we recently introduced [9]. In our scheme, the transmission band of each link on the route can be adapted in consideration of GSNR performance, which can lead to margin reduction and network performance improvement. Demonstrating its potential benefits, we present numerical results to show that our scheme enables accommodated traffic volume to be increased by more than 30% compared to conventional adaptation schemes. We also discuss the impact of physical-layer performance of band switching operations on the available network capacity to investigate the feasibility of the proposed scheme.

978-3-903176-33-1 

## II. Multi-Band Optical Network with Wavelength-Selective Band Switching

For this paper, we assume the S+C+L-band optical network comprised of standard single-mode fiber (SSMF) links and MB optical cross connect (MB-OXC) nodes enabling wavelength-selective band switching. Two examples of possible MB-OXC architecture are schematically depicted in Fig. 1. As shown in Fig. 1(a), one example is a primitive architecture that employs wavelength selective switch (WSS) for each band. In addition to WSSs and band (de)multiplexers, all-optical wavelength converters (AO-WCs) are employed for band switching operations. Specifically, such AO-WCs are assumed to be able to convert the transmission band, as a recent experiment was conducted in which multiple-wavelength conversion operations

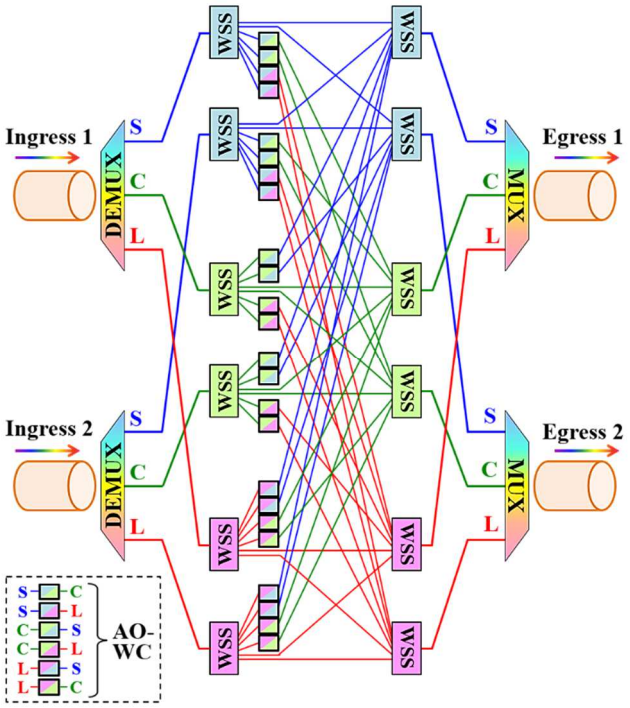


(a) Primitive architecture employing WSS for each band

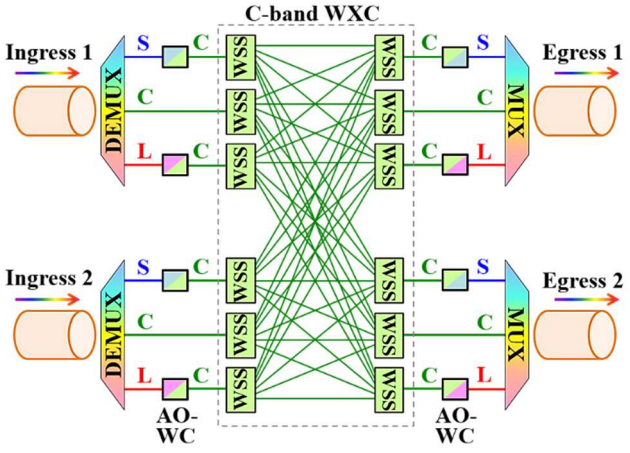


(b) Common-band WSS-based architecture

Fig. 1. Possible architectures of MB-OXC node that enable wavelength-selective band switching (in the case of 2-degree node).

"from/to C-band to/from L-band" and "from/to C-band to/from S-band" were successfully demonstrated [10]. Consequently, this MB-OXC enables each incoming wavelength channel to be output to any direction on any band; namely, it enables band switching to be realized. The other is a common-band WSS-based architecture that we recently proposed [9]. This architecture also utilizes AO-WCs, as shown in Fig. 1(b). Thanks to the placement of ingress and egress AO-WCs, the wavelength cross connect (WXC) function can be implemented with arbitrary single band components. Specifically, in Fig. 1(b), AO-WCs convert the spectrum from/to S- or L-band to/from C-band, and C-band signals are handled by a WXC implemented only with C-band WSSs. Just as the former, each wavelength channel on each band can be freely switched to any band and direction.

Key components of these MB-OXC are AO-WCs that enable wideband and multiple-wavelength conversion as well as modulation format/bit-rate agnostic operation. Note that AO-WCs are becoming available thanks to recent progressive efforts [10–13]. For instance, a practical and compact device for AO-WC based on periodically poled lithium niobate (PPLN) waveguides or highly-nonlinear fibers (HNLFs) can be deployed in MB-OXC nodes. Moreover, it is worth noting that WSS-related technologies have also been extensively investigated, which allows to cost-effectively implement MB-OXC nodes. For instance, a primitive architecture can naturally make use of MB WSSs for hardware scale reduction [14]. In addition, by applying multiple-arrayed WSS technologies [15, 16], multiple C-band WSSs can be integrated into a single optics system, which enables a common-band WSS-based architecture to be implemented in a hardware-efficient manner. Furthermore, although several other technology options can be applied, such investigation in MB-OXC architecture is beyond the scope of this paper. In particular, this paper focuses on the MB network performance in terms of the traffic volume that can be accommodated.

Originally, the essential role of an optical network is to provide guaranteed connectivity to client systems such as routers by provisioning optical paths. For provisioning such a path in response to a connection request, network resource in terms of optical spectrum on the fiber link must be assigned exclusively. To maximize the MB network performance, spectrum resources must be efficiently utilized in consideration of transport margin. Moreover, many factors must be taken into consideration in path provisioning. Specifically, such factors include the SRS effect and several physical parameters; each band generally has a different fiber attenuation and the amplifier noise figures vary when a different amplifier is applied to each band. Furthermore, the transport margin must be efficiently managed in consideration of attainable GSNR performance over the multiple bands, especially on a large-scale MB network. In fact, on a small-scale network, the transport margin can be easily managed even in MB operations because the variation of path length tends to be small. In contrast, a large-scale network generally has a larger variation of path length, and the margin shortage of the longest path must be avoided. If a number of paths have large margins, redundant resources tend to be assigned and the potential of the MB network is underutilized, which can lead to a decrease in the acceptable traffic volume.

Therefore, further investigation on MB network performance needs to be tackled with a novel approach towards the optical-layer adaptation for low margin networking.

## III. Adaptive Link-by-Link Band Allocation

The aim of adaptive link-by-link band allocation is to attain the desired GSNR performance at the receiver end in a spectrum-efficient manner. For each path, according to physical conditions (i.e., GSNR performance) on the route, the set of bands on each link is selected based on specific criteria such as minimizing the difference between the actual GSNR and minimum GSNR required for a given error rate (GSNR margin).

We illustrate the principle of our scheme by contrasting it with a conventional scheme in Fig. 2, where three bands are supported and optical paths are provisioned with a common single modulation format (e.g., dual-polarization quadrature phase-shift keying (DP-QPSK)). Note that histograms of the attainable values of received GSNR are shown on the right in Fig. 2. In an end-to-end band allocation scheme, once the band is selected, the received GSNR can be determined for a particular route. Also note that the value depends on the path length, and the GSNR histogram tends to show wide distribution like that in Fig. 2(a). Moreover, spectrum on each band must be treated as separated and independent resources. In such cases, high margins tend to be allocated to paths on better-performing bands, while worse-performing bands can cause margin shortage. On the other hand, in our scheme, the band on each link can be treated as a parameter for adapting the attainable GSNR. This is thanks to wavelength-selective band switching [9], which enables each optical channel to be switched to any band and direction in the optical layer. This enables the band on each link to be freely switched without the need for costly and power-hungry 3R regenerators which are utilized in opaque or translucent networks. By using information on GSNR performance per span for each band, the attainable GSNR at the receiver end can be estimated for any combination of bands, according to [17]. Note that both amplified spontaneous emission (ASE) noise generated by optical amplifiers and nonlinear interference (NLI) generated in fiber propagation are considered when estimating GSNR. Consequently, the received GSNR can be closely matched to a particular threshold in response to the path-length distribution and the variation in the amount of GSNR degradation, enabling both low-margin operations and avoiding margin shortage as shown in Fig. 2(b).

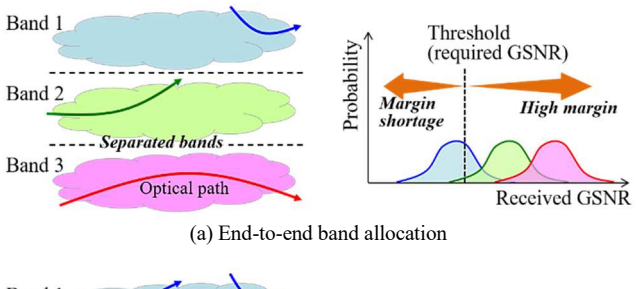


Fig. 2. Principles of band allocation schemes.

To activate our novel adaptation scheme in optical network operations, we present a heuristic path provisioning algorithm utilizing adaptive link-by-link band allocation. For each path, this algorithm first lists all possible band combinations for each link, estimates received GSNR for each combination, and then determines the one with the lowest possible GSNR margin. As shown in Fig. 3, it is executed as follows. Now, suppose that

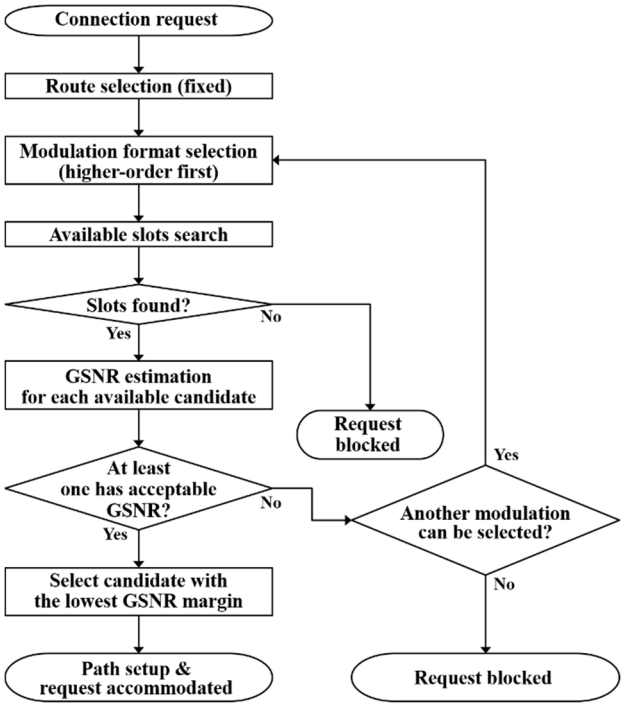


Fig. 3. Flowchart of path-provisioning algorithm.

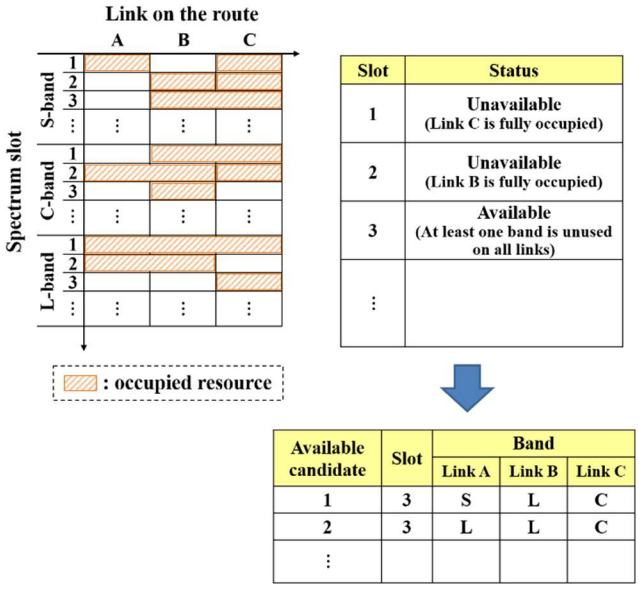


Fig. 4. Example of available slots and candidates in path provisioning.

spectrum resources on each band are divided into 12.5-GHz slots and numbered, and single-span GSNR for each band is known in advance or pre-calculated. In response to a connection request, the fixed shortest route is simply applied to guarantee low latency by avoiding detouring, and the highest-order modulation format is chosen when multiple modulation formats are supported in order for efficient spectrum utilization. Then, the available slots of which at least one band is unused on all the links are searched, as illustrated in Fig. 4. Next, for each available slot, the received GSNR is calculated for each available candidate, i.e., each combination of the unused bands on each link. Afterwards, the candidate that has the lowest GSNR margin is selected. If multiple candidates attain the same margin, the lower-numbered one is determined, and path is setup to accommodate the request. On the other hand, if no candidate satisfying the above conditions can be found, a lower-order modulation format is chosen and computation is retried. If these retries fail with all modulation format candidates or there are no spare resources available, the request is blocked.

## IV. Numerical Evaluation

To numerically verify the benefits of a novel adaptation achieved with our scheme in comparison with conventional adaptation schemes, we conduct realistic simulations. In the followings, we first describe the assumed network model including physical parameters. Second, we investigate the maximum potential benefits of the adaptive link-by-link band allocation in terms of network performance improvement. Then, the impact of physical-layer performance of band switching operation on network performance is discussed to explore the feasibility of the proposed adaptation scheme.

### *A. Network Model*

We assume that L- and S-bands are exploited in addition to C-band, as described in Sec. II, which is a possible option for a core network due to the relatively low loss properties. The physical topology tested is NSFNET [18], as shown in Fig. 5. This topology has 14 nodes and 21 bidirectional links where the average link length is 1080 km and a span length of 100 km is assumed. On each link, spectrum resources of 4.7, 4.3, 4.6 THz are available in the S-, C-, and L-bands, respectively, as shown in [2].

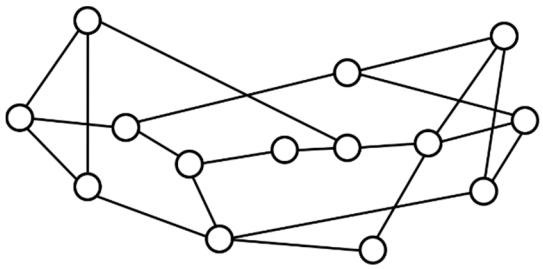

Fig. 5. NSFNET topology.

TABLE I. Per-Band Worst-Case GSNR after 100-km Single Span Transmission

| Scenario | S-band | C-band | L-band |
|---|---|---|---|
| C-band only | – | 24.38 dB | – |
| S+C+L-band | 17.45 dB | 22.26 dB | 23.9 dB |

Physical parameters of each link are assumed as follows. The attenuation coefficient, dispersion, dispersion slopes, nonlinear coefficient, and Raman gain slopes are 0.22 dB/km, 17 ps/nm/km, 0.067 ps/nm2/km, 1.2 1/W/km, and 0.05 1/W/km/THz, respectively. At the end of each span, the span loss and the spectral tilt induced by SRS are compensated by an erbium-doped fiber amplifier (EDFA) with noise figures of 5 and 6 dB for the C- and L-bands, and a thulium-doped fiber amplifier (TDFA) with noise figure of 7 dB for S-band, respectively. The fiber launch power per channel is set to 0 dBm, and the estimated worst-case GSNR values after a 100-km single span transmission under assumed condition are summarized in Table I. Note that this launch power setting aims to suppress GSNR degradation of better-performing bands, which enables long-distance paths to be setup with sufficient quality. Also note that the full traffic load is assumed in GSNR estimation in which the applied procedure is based on the recent work [17]. Although this assumption may be conservative, this can exclude the impact of path addition during path provisioning. More specifically, every existing path can attain sufficient performance when any new path is setup.

In our simulation, end-to-end optical paths are provisioned by assigning spectrum resources, in response to connection requests. Such requests are assumed to arrive sequentially and to have an infinite holding time. Request arrival follows uniform random distribution, and each request has 100 Gbps capacity. Moreover, the modulation formats used are 16 Gbaud DP 16-ary quadrature amplitude modulation (DP-16QAM), 32 Gbaud DP-QPSK, and dual-carrier 32 Gbaud DP binary phase-shift keying (DP-BPSK) for guaranteeing 100-Gbps capacity, and each format requires spectrum resources of 25, 50, and 100 GHz, respectively. According to [19], assuming the pre-forward error correction (FEC) bit error rate (BER) limit of $2\times10^{-2}$, the threshold values of GSNR are assumed to be 13.8, 7.2, and 4.2 dB for DP-16QAM, DP-QPSK, and DP-BPSK, respectively.

Comparisons of network performance are provided among four scenarios: (i) single-modulation (DP-QPSK) network with end-to-end band allocation, (ii) multi-modulation network with end-to-end band allocation, (iii) single-modulation (DP-QPSK) network with adaptive link-by-link band allocation, and (iv) multi-modulation network with adaptive link-by-link band allocation. Note that the end-to-end band adaptation presented in [8] is applied to scenarios (i) and (ii). Also note that scenarios (ii) and (iv) can utilize modulation format adaptation.

### *B. Benefits of Adaptive Link-by-Link Band Allocation*

The blocking probability as a function of the number of offered connection requests are shown in Fig. 6, where each result is obtained by averaging 10000 simulation runs. Please note that GSNR penalty resulting from band switching is not considered in Fig. 6 for investigating the maximum potential benefits of the adaptive link-by-link band allocation. The results reveal that our proposed scheme can significantly enhance network performance. For instance, when the target blocking probability is 0.01, our scheme allows accommodated requests to be increased by more than 30% compared to conventional adaptation schemes, which is a remarkable gain achieved by a novel optical-layer adaptation. This implies that our scheme can successfully allocate appropriate margins to each path and can

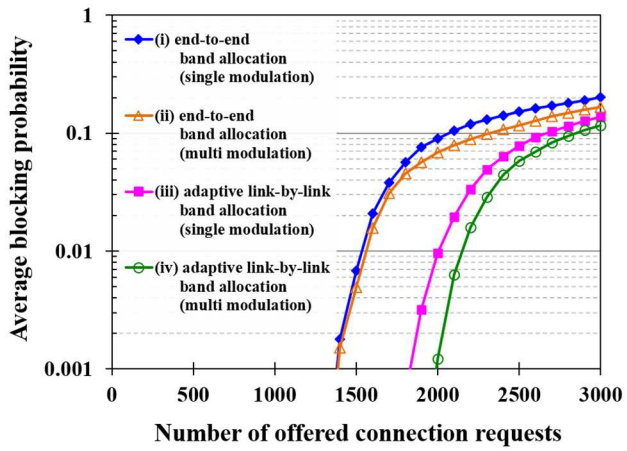


Fig. 6. Blocking performance of each scenario.

save spare resources for the later requests. Moreover, scenario (iv) exhibits the best result, and this scenario can accommodate about 45% more traffic than conventional ones. This is mainly because fine-granularity adaptation can provide a GSNR performance close to the threshold. In addition, it should be emphasized that the adaptive link-by-link band allocation enables a single-modulation scenario (iii) to attain better performance compared to a multi-modulation scenario (ii) without increasing hardware complexity of TRs, which are generally the dominant cost factor in large-scale optical networks as a large number of TRs are deployed. As a result, our scheme can cost-effectively improve network performance through appropriate use of spectrum resources over existing fiber infrastructure.

Furthermore, to quantify the reduction of GSNR margin achieved with our scheme, histograms of GSNR margins allocated to established paths are shown in Fig. 7, when the number of offered requests is 2000. With an adaptive link-by-link band allocation scheme, about 1 dB of GSNR margin can be reduced on average, compared to a conventional end-to-end band allocation scheme. Also, more than 90% of paths can attain a GSNR margin of less than 1 dB with our scheme, which successfully demonstrates that low-margin MB networking can be realized.

### C. *Impact of GSNR Penalty Induced by Band Switching*

To clarify the viability of our proposed scheme, we here evaluate the network performance in consideration of the GSNR penalty induced by the band switching operation. In fact, the transmission penalty arising from AO-WCs and its actual impact on network performance are of great concern for practical use. Generally, physical-layer performance of AO-WCs depend on the mechanism for wavelength conversion, optical device specifications and implementation. In this evaluation, GSNR penalty per band switching operation is introduced as a parameter in GSNR estimation. Specifically, a band switching induced GSNR penalty and the number of such operations are considered in Fig. 3, where the sum of GSNR penalties is simply subtracted from original attainable GSNR value. Please note that the node configuration in Fig. 1(a) is assumed. The acceptable traffic volume with a target blocking probability of 0.01 is derived for scenarios (iii) and (iv) and normalized by scenario

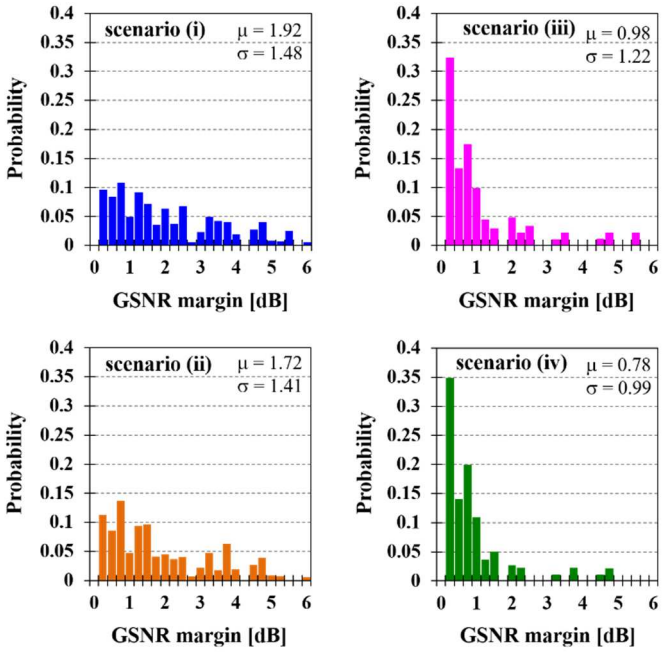


Fig. 7. Histograms of attained GSNR margins.

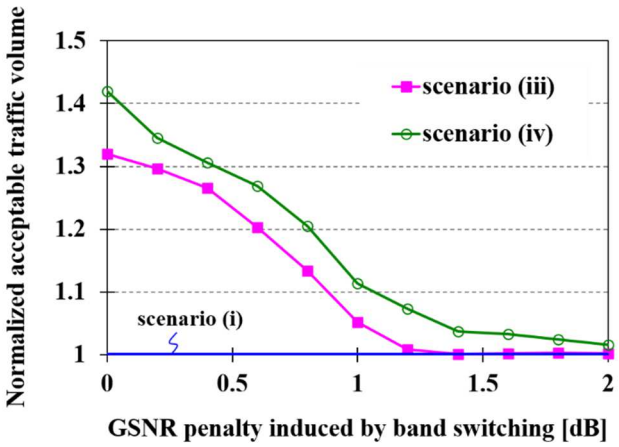


Fig. 8. Impact of GSNR penalty induced by band switching operation on network performance.

(i), as shown in Fig. 8. This normalized traffic volume can be regarded as the performance gain achieved by our adaptation scheme. The results indicate that a large gain can be obtained even when the band switching induced GSNR penalty is considered. For instance, a performance gain of more than about 25% can be achieved if GSNR penalty per band switching is suppressed lower than 0.5 dB. Please note that GSNR penalty of 0.5 dB may be a possible value, because in recent experiments (see [9]), we observed a Q-penalty of less than 0.5 dB in a particular band switching configuration and such a Q-penalty is generally comparable to the GSNR penalty near FEC limit.

Also, in the literature, several highly-efficient AO-WCs have been proposed and their physical performance has been extensively studied. For instance, the performance of an HNLF-based AO-WC has been intensively evaluated in [12, 20].

Specifically, in [12], converting operation of multiple wavelength channels with different modulation formats including DP-QPSK and DP-16QAM have been successfully demonstrated without significant degradation in transmission quality. In addition, experiments in [12] have also shown that AO-WC performance was not affected by the amount of wavelength shift (i.e., difference in wavelength between input and output signals). Such results prove the feasibility of wideband, multiple-channel and modulation-format-agnostic AO-WC operations. Moreover, in [20], it has been demonstrated that an HNLF-based AO-WC exhibits a low noise figure and low phase noise, and thus it is cascadable as an EDFA. Indeed, such cascadability is an important metric of AO-WCs, and is strongly affected by the conversion efficiency. In [21], the impact of conversion efficiency of AO-WCs on transmission performance has been studied where DP-16QAM signals and an HNLF-based AO-WC are assumed to be used. Furthermore, conversion efficiency of AO-WCs based on PPLN devices have also been discussed in [11, 13]. According to [11], mainly due to low insertion loss and sufficient parametric conversion gain, a PPLN-based AO-WC has the potential of lossless operation. Note that lossless operation of AO-WCs can naturally minimize the GSNR penalty induced by band switching operations and maximize performance gain. In consequence, such efforts will increase practicality and reliability of wavelength-selective band switching. Moreover, advances in AO-WC technologies can boost MB optical network performance with our proposed adaptation scheme.

## V. Conclusions

We proposed and investigated a novel approach towards fine-granularity adaptation on multi-band optical networks, in which the attainable received GSNR can be finely adapted. The proposed adaptation scheme can attain low-margin operations by adaptively allocating the transmission band of each link on the route in consideration of the attainable GSNR performance. The obtained numerical results demonstrated that a remarkable reduction in GSNR margin can be achieved and potentially enable a more than 30% increase in accommodated traffic volume compared to conventional adaptation strategies. We also discussed the feasibility of our scheme. The proposed scheme will introduce a new degree of optical-layer adaptation and open the opportunity for further advancement in multi-band optical networking.

## References


[1] A. Napoli, N. Calabretta, J. K. Fischer, N. Costa, S. Abrate, J. Pedro, V. Lopez, V. Curri, D. Zibar, E. Pincemin, S. Grot, G. Roelkens, C. Matrakidis, and Wladek Forysiak, "Perspectives of multi-band optical communication systems," Proc. OECC 2018, paper 5B3-1, July 2018.

[2] F. Hamaoka, M. Nakamura, S. Okamoto, K. Minoguchi, T. Sasai, A. Matsushita, E. Yamazaki, and Y. Kisaka, "Ultra-wideband WDM transmission in S-, C-, and L-bands using signal power optimization scheme," J. Lightw. Technol., vol. 37, no. 8, pp. 1764–1771, Apr. 2019.

[3] N. Sambo, A. Ferrari, A. Napoli, N. Costa, J. Pedro, B. Sommerkorn-Krombholz, P. Castoldi, and V. Curri, "Provisioning in multi-band optical networks," J. Lightw. Technol., vol. 38, no. 9, pp. 2598–2605, May 2020.

[4] A. Ferrari, A. Napoli, J. K. Fischer, N. Costa, A. D'Amico, J. Pedro, W. Forysiak, E. Pincemin, A. Lord, A. Stavdas, J. P. F.-P. Gimenez, G. Roelkens, N. Calabretta, S. Abrate, B. Sommerkorn-Krombholz, and V. Curri, "Assessment on the achievable throughput of multi-band ITU-T G.652.D fiber transmission systems," J. Lightw. Technol., vol. 38, no. 16, pp. 4279–4291, Aug. 2020.

[5] D. Uzunidis, C. Matrakidis, A. Stavdas, and A. Lord, "Power optimization strategy for multi-band optical systems," Proc. ECOC 2020, paper Tu1H-4, Dec. 2020.

[6] J. Slovak, M. Herrmann, W. Schairer, E. Torrengo, K. Pulverer, A. Napoli, and U. Häbel, "Aware optical networks: Leaving the lab," J. Opt. Commun. Netw., vol. 11, no. 2, pp. A134–A143, Feb. 2019.

[7] M. Jinno, "Elastic optical networking: Roles and benefits in beyond 100-Gb/s era," J. Lightw. Technol., vol. 35, no. 5, pp. 1116–1124, Mar. 2017.

[8] M. Nakagawa, H. Kawahara, K. Masumoto, T. Matsuda, and K. Matsumura, "Performance evaluation of multi-band optical networks employing distance-adaptive resource allocation," Proc. OECC 2020, Oct. 2020.

[9] H. Kawahara, M. Nakagawa, T. Seki, and T. Miyamura, "Experimental demonstration of wavelength-selective band/direction-switchable multi-band OXC using an inter-band all-optical wavelength converter," Proc. ECOC 2020, paper Tu1H-5, Dec. 2020.

[10] T. Kato, S. Watanabe, T. Yamauchi, G. Nakagawa, H. Muranaka, Y. Tanaka, Y. Akiyama, and T. Hoshida, "Real-time transmission of 240×200-Gb/s signal in S+C+L triple-band WDM without S- or L-band transceivers," in Proc. ECOC 2019, paper PD.1.7, Sept. 2019.

[11] T. Umeki, O. Tadanaga, and M. Asobe, "Highly efficient wavelength converter using direct-bonded PPZnLN ridge waveguide," IEEE J. Quantum Electron., vol. 46, no. 8, pp. 1206–1213, Aug. 2010.

[12] K. Ishii, T. Inoue, I. Kim, X. Wang, H. N. Tan, Q. Zhang, T. Ikeuchi, and S. Namiki, "Analysis and demonstration of network utilization improvement through format-agnostic multi-channel wavelength converters," J. Opt. Commun. Netw., vol. 10, no. 2, pp. A165–A174, Feb. 2018.

[13] C. Wang, C. Langrock, A. Marandi, M. Jankowski, M. Zhang, B. Desiatov, M. M. Fejer, and M. Lončar, "Ultrahigh-efficiency wavelength conversion in nanophotonic periodically poled lithium niobate waveguides," OSA Optica, vol. 5, no.11, pp. 1438–1441, Nov. 2018.

[14] K. Seno, K. Yamaguchi, K. Suzuki, and T. Hashimoto, "Wide-passband C+L-band wavelength selective switch by alternating wave-band arrangement on LCOS," Proc. ECOC 2018, paper We1C.6, Sept. 2018.

[15] H. Yang, B. Robertson, P. Wilkinson, and D. Chu, "Small phase pattern 2D beam steering and a single LCOS design of 40 1 × 12 stacked wavelength selective switches," Opt. Express, vol. 24, no. 11, pp. 12240–12253, May 2016.

[16] K. Suzuki, K. Seno, and Y. Ikuma, "Application of waveguide/free-space optics hybrid to ROADM device," J. Lightw. Technol., vol. 35, no. 4, pp. 596–606, Feb. 2017.

[17] D. Semaru, R. I. Killey, and P. Bayvel, "A closed-form approximation of the Gaussian noise model in the presence of inter-channel stimulated Raman scattering," J. Lightw. Technol., vol. 37, no. 9, pp. 1924–1936, May 2019.

[18] P. Yi and B. Ramamurthy, "Provisioning virtualized cloud services in IP/MPLS-over-EON networks," Photon. Netw. Commun., vol. 31, no. 3, pp. 418–431, Dec. 2015.

[19] X. Zhou and C. Xie, "Enabling technologies for high spectral-efficiency coherent optical communication networks," Wiley Series in Microwave and Optical Engineering, Apr. 2016.

[20] H. N. Tan, T. Inoue, K. Solis-Trapala, S. Petit, Y. Oikawa, K. Ota, S. Takasaka, T. Yagi, M. Pelusi, and S. Namiki, "On the cascadability of all-optical wavelength converter for high-order QAM formats," J. Lightw. Technol., vol. 34, no. 13, pp. 3194–3205, July 2016.

[21] T. Yamauchi, T. Kato, G. Nakagawa, S. Watanabe, Y. Akiyama, and T. Hoshida, "Investigation on maximum transmission reach in wavelength converted systems," Proc. OECC/PSC 2019, paper WB3-3, July 2019.